INSTABILITY DEVELOPMENT IN TWO-PHASE SHEAR FLOWS: PRIMARY BREAKUP

P. Yecko and S. Zaleski**

**Laboratoire de Modélisation en Mécanique, Université Pierre et Marie Curie (Paris VI)*
4, place Jussieu, Tour 66, 75252 Paris Cedex 05, France

ABSTRACT: We examine the development of instability for a shear flow made up of two distinct immiscible fluids, taking into account their disparate densities, viscosities and the possibility of tension acting on the interface that separates them. The most unstable mode found by linear theory is believed to explain the instability of breakup at its onset. We also find a second mode, which can be most unstable in certain situations of interest. Direct numerical simulations are performed for a range of densities, viscosities and Reynolds numbers. At early times, simulations recover the amplitude growth predicted by linear theory, verifying the applicability of the numerics for breakup simulations; at later times, the models show the development of elongated structures and the subsequent breakup of the heavier fluid into drops.

INTRODUCTION

This study examines the instability of liquid breakup at early times. In the atomization process, there is a general picture which traces the initial growth of wave-like disturbances into more elongated sheets of heavier fluid penetrating into the lighter fluid. Out of these sheets, ligaments, or fingers, grow and ultimately break into droplets [1].

Numerically, we simulate this process over a wide range of densities and viscosities, verfying the code by comparison with linear theory. We use an existing algorithm (SURFER) of the Volume of Fluid type with Piecewise Linear Interface Construction (VOF/PLIC), which is designed for accurate simulations of flows with tense surfaces [2].

parallel flow examined here. The lower layer is denoted by the index $i = 1$, which will be taken to represent the more dense fluid, and will sometimes be referred to as the "liquid" while the upper layer, $i = 2$, will be referred to as the "gas." The densities, ρ_i, and the dynamic viscosities, μ_i will, in general, have different values in the different layers. The layer interface, represented by the horizontal line separating the two regions, is initially flat. At the top and bottom of the domain are rigid walls, while we will assume periodicity in the x, or down-stream direction. The velocity, a classic parallel flow, varies only in the y, or cross-stream, direction, and is continuous across across the interface. The y-derivative of the velocity, however, will experience a discontinuity whose magnitude is proportional to the ratio of the viscosities, as demanded by the continuity of tangential stress across the interface. Further aspects of the flow will depend on the particular choices of the functions $U_i(y)$ given below.

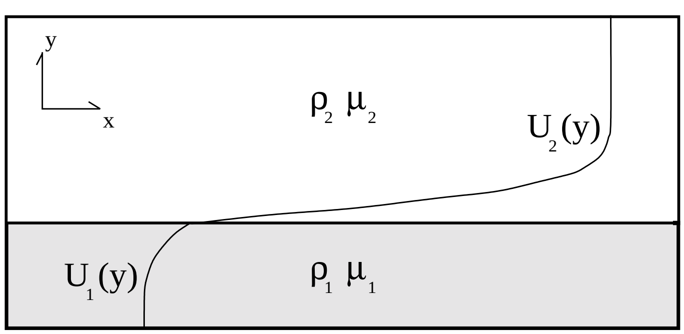

Figure 1: A schematic representation of the shear flow under study.

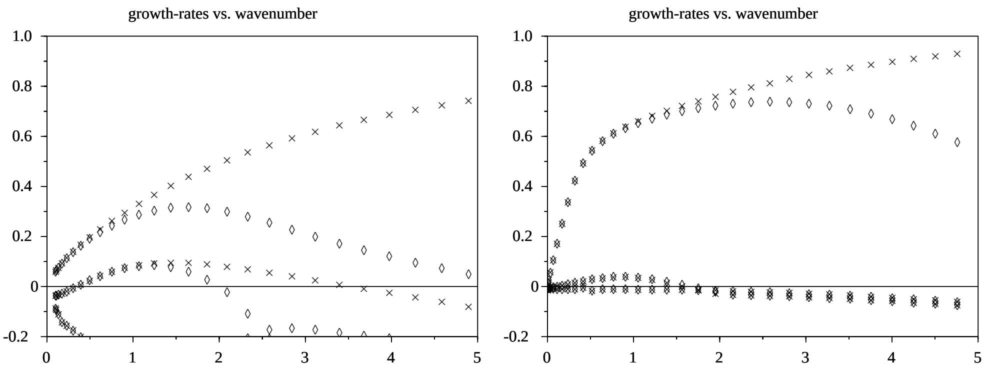

Figure 2: Most unstable mode growth-rates for air-water (left) and the simulation case (right). Shown are the values of αc_i plotted as a function of the wavenumber α. The horizontal line at $y = 0$ separated the unstable modes, above the line, from the damped modes below. Two calculations are superposed: with no surface tension (x's) and for $We = 100$ (diamonds).

LINEAR THEORY

The incompressible Navier-Stokes equations are our basis for linear perturbation theory. Special interface conditions are used, since surface tension may act, and gravity may be felt there.

Basic state

The two-layer system is linearized around the basic state given by:

$$U_2(y) = \quad U_2^* \; erf(y/\delta_2) \qquad y > 0 \tag{1}$$
$$U_1(y) = \quad U_1^* \; erf(-y/\delta_1) \qquad y < 0 \tag{2}$$

This flow represents a laminar boundary layer flow in each layer, having characteristic thickness scale δ_i and characteristic velocity U_i^* far from the interface. In the limit $\delta_i \to 0$, the boundary layer thicknesses approach zero, and the velocity profiles approximate that of the classic Kelvin-Helmholtz layer, or vortex sheet, but in a bounded viscous flow.

Linear results in the air-water and model regimes

To solve the linear eigenvalue problem, we represent the eigenfunction by an expansion in Chebyshev polynomials and employ a collocation method to arrive at a linear system for the expansion coefficients. This technique is known to give very accurate eigenvalues for many parallel flow problems, using a minimal spectral resolution [3].

Since the problem we are most interested in –the breakup and atomization of a liquid layer– is also realized in the air-water regime, we will take the air and water case as a reference point for the calculations performed here. We also calculate the properties of two nonexistent fluids whose density and viscosity ratios are more modest than those of air and water, and which are ideal when making direct numerical simulations. Results in both cases will initially be presented in tandem.

We have verified that the nature of the instability is not dependent on the presence of walls by varying the positions of the walls and verifying the robustness of the unstable modes, a characteristic also alluded to by Hooper and Boyd [4]. The walls are maintained in order to have compatibility with the numerical simulations to be performed later.

Parameter values

Calculations here are confined to a small subset of possible parameters as follows: α is varied between zero and 2π, $Re = 400$, $Fr = \infty$ and $We = 100$. Furthermore, $n = 1$ for all calculations here. For the air-water problem, we adopt the actual density ratio: $r = 0.0012$; and the actual viscosity ratio: $m = 0.012$. For the simulations we use the more modest values: $r = 0.1$, and $m = 0.1$. We have neglected the presence of gravity ($Fr = \infty$), having verified its negligibility on the results when $Re = 400$.

In Fig. 2 we show the growth-rates (αc_i) of the most unstable modes over a range of α for $Re_l = 400$. We show results with and without surface tension in both cases, as explained in the figure. What is most noteworthy is the fact that there are two unstable modes coexisting at small values of α, for both parameter sets.

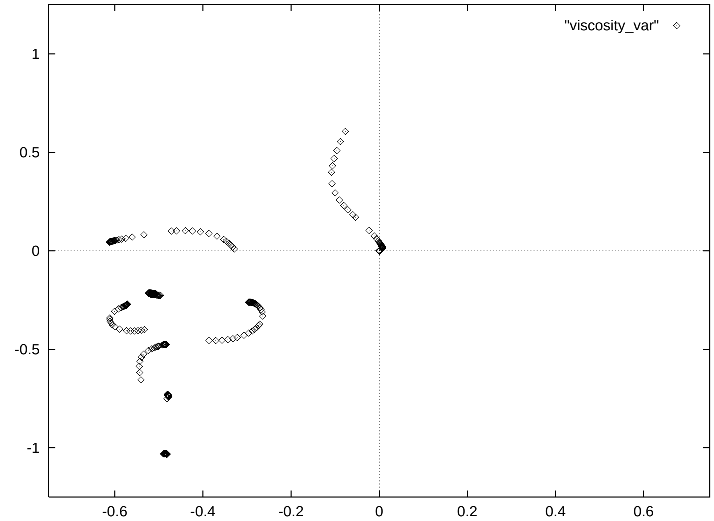

Figure 3: Mode crossing for fixed $\alpha = 1$ and variable m, plotted in spectral coordinates here. The interfacial mode and vortical mode occupy the same regions as before, but here, as $m \to 1$, the growth-rate of the vortical mode moves down, always decreasing, while that of the vortical mode moves to the left in the figure, first increasing and only later decreasing. In the intermediate range, the vortical mode is more unstable.

For brevity, we refer to the more unstable of these two modes as the interfacial mode and to the other the vortical mode. Miesen et al. [5] and Hooper [6] have also noted the presence of two modes in related problems, though the exact nature of their distinction is still not well accounted.

Up to wavenumbers α in the range 1.5–2.0, the effect of surface tension is slight. At higher wavenumbers, its effective stabilization of the most unstable modes is apparent in Fig. 2. More importantly, it leads to an upper cutoff for instability which falls within the accessible dynamic range of the numerical simulations. The stabilizing effect of surface tension seems to be more effective on the more unstable of the two modes, the interfacial mode.

Boundary layer vorticity distribution

By varying parameters, the growth-rates of the of the interfacial and vortical modes will vary such that either of the two modes can be the most unstable over a range of α. The effect that leads to such *mode crossings* in this problem is linked to the relative distributions of the vorticity in layers, but especially in the liquid layer.

The viscosity ratio seems to be (and has been previously identified as [6]) the dominant factor of the instability in this context, but this dependence arises indirectly. Recall that the vorticity is discontinuous if the dynamic viscosity is not the same for the two fluids. For fixed boundary layer thicknesses, the viscosity ratio is therefore linked to the vorticity gradient of the flow. There are particular combinations of parameter choices that can lead to equivalent vorticity distributions, and therefore to equivalent modal behavior, for that part of the spectrum which depends on the vorticity distributions. This is more simply expressed by noting that the following relation must hold for the configuration we have adopted: $U_2^*/U_1^* = n/m$.

It is therefore possible to demonstrate the effect of altering the relative vorticity distribution by altering the viscosity ratio m, the layer thickness ratio n or the velocities. Mode crossing is especially evident in spectral coordinates: in Fig. 3 we show a variation of m from 0.001 (the bottom-most point of the interfacial mode track and the left-most point of the vortical mode track) to a value of 0.1 (the opposite end of both tracks). Over a certain range of intermediate values, the vortical mode remains the most unstable.

The mode crossing Fig. 3 figure illustrates that the two modes have a different physical character, but does little to illuminate the nature of that difference. Instead, we can look at the distribution of the work integrand associated with the Reynolds stresses through the flow (Fig. 4).

$$P(y) = \int_{-h_l}^{h_g} \tau \frac{du}{dy} dy \tag{3}$$

where $\tau(y) = \phi_r D_y \phi_i - \phi_i D_y \phi_r$.

In a real flow, there is typically a development of the boundary layer, possibly involving flow reversals, which could lead to explosive growth of either mode.

Raynal [7] has identified the existence of two modes and argued that the gas mode is dominant. We argue that the so-called liquid mode has a growth rate (work integrand) that depends sensitively on the ratio of viscosities and/or the ratio of boundary layer thicknesses, and so can overpower the interfacial mode in cases.

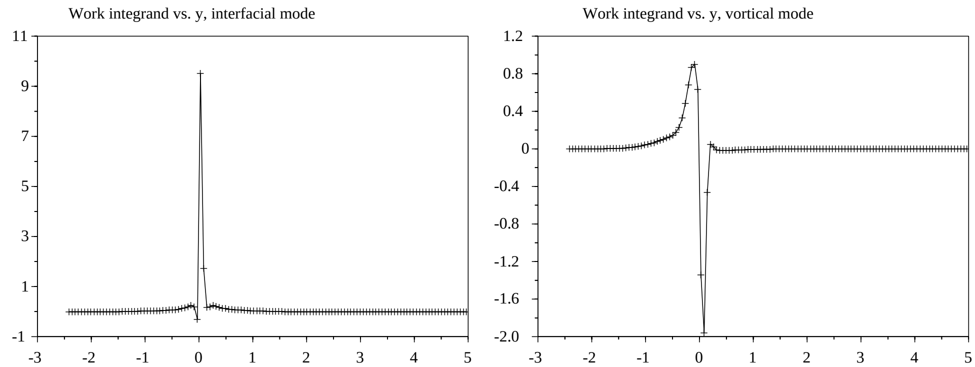

Figure 4: Reynolds-stress work integrand $P(y)$ vs. y for the interfacial mode (left), and vortical mode (right). Integrated across the channel (left to right here), this gives the growth rate of the mode.

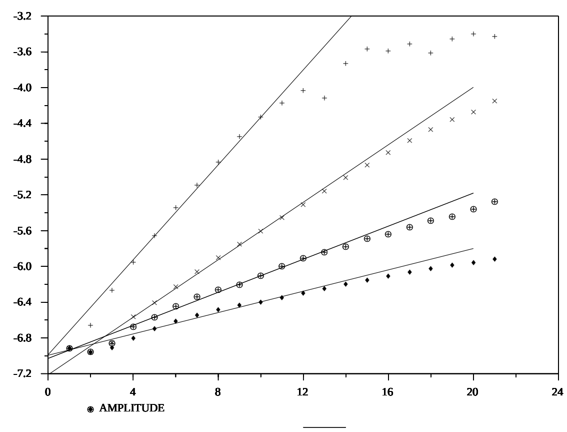

Figure 5: Comparison between amplitude growth as extracted from the simulations (points) vs. the predicted growth-rates of linear theory (solid lines). The three lower curves reflect three different values of the density ratio, $r = 0.05, 0.01, 0.005$ from bottom to top, while the uppermost curve is for $r = 0.02$, representative of the SEP Vulcain rocket engine; note that there is a different characteristic time-scale in this case.

NONLINEAR RESULTS

The SURFER algorithm is well documented [2], so we mention here just that the so-called *spurious current*, introduces numerical error that we wish to verify the insignificance of here. In all model runs we have used a mesh of 128 grid points square (verification runs were performed up to 512-square resolution), and the same flow parameters as for the linear theory, given above.

Simulations in the linear regime

Initial perturbations of two types were used: in one case, an simple noisy initial condition was used while in the other case, a perturbation having the structure of the most unstable eigenmode was used.

When beginning the calculation with a superposition of the unstable eigenfunction found from linear theory and the basic state flow, we see an initial adjustment period. This apparently results from the inability to resolve the variations of the interface position of arbitrarily small magnitude when the entire variation is smaller than one mesh point. In fitting the growth rates, the behavior of the amplitude in this adjustment phase is ignored.

Following the adjustment, the instability subsequently grows as a pure exponential, following the predicted linear growth-rate over approximately two orders of magnitude in amplitude.

It is also worthwhile to perturb the basic state flow in such a way that the most unstable eigenfunction appears naturally. To do this, we form an initial noisy perturbation from a superposition of all modes resolvable on the numerical mesh, and randomize their phases in both spatial dimensions (similar to initial conditions often employed in two-dimensional turbulence decay simulations). After an initial transient resulting from the decay of the many superposed damped modes excited by the initial condition, the most unstable mode appears immediately and begins its exponential growth.

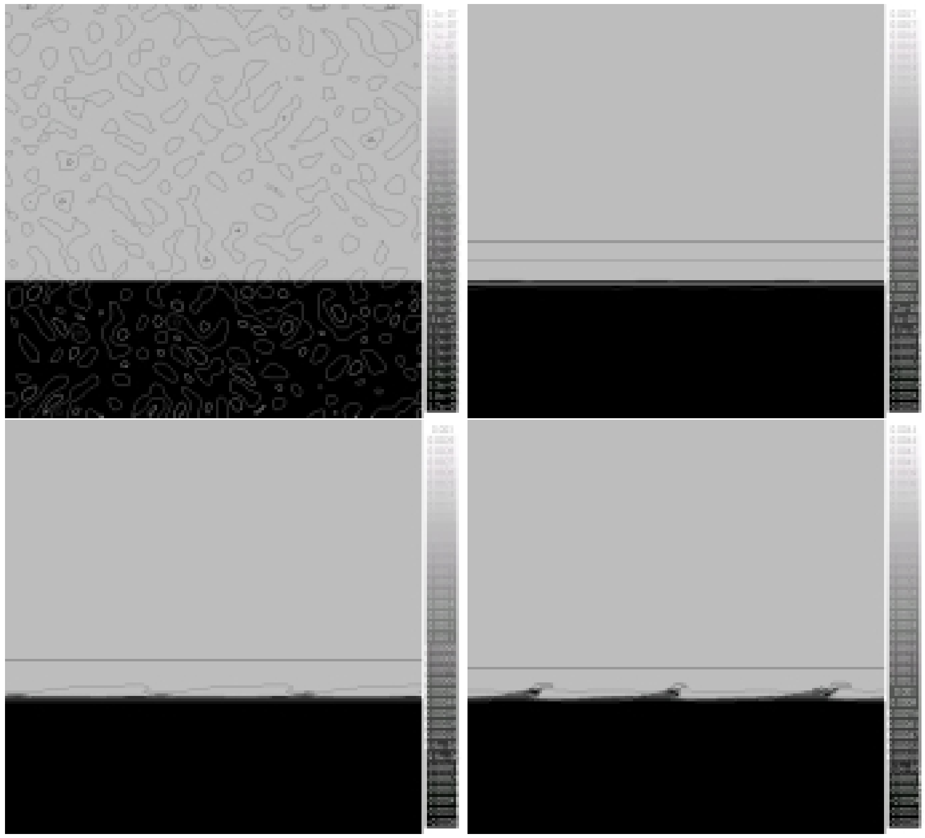

Figure 6: Evolution of the two-phase flow, as before, but here $r = 0.02$ and the initial condition visible in the top right frame shows the vorticity of the noisy initial condition.

Its rate of growth sticks to the value predicted by the linear theory, again over approximately two orders of magnitude in the amplitude, but typically more. In Fig. 5 we show the comparison between the growth-rates that appear in the simulations and those calculated by linear theory. For the purpose of verifying the efficacy of the code at stronger density ratios, we have repeated this check for a range of densities, as given in the figure. Since the agreement of numerical simulations and linear theory is very good over several orders of magnitude (these figures employing a Log_{10}-scale) for even the more challenging density ratios, we conclude that the numerical method is valid in these regimes. We also note that previous discrepancies between the growth-rates of simulations and from linear theory were mostly a consequence of the comparison to a particular linear theory (inviscid, piece-wise continuous velocity profiles) that does not remain valid in the viscous code long enough to follow several orders of magnitude of amplitude growth – viscous boundary layers form and grow even at the largest simulation Reynolds numbers, and the resulting flow evolution implies a variable growth-rate of the most unstable mode.

Simulations in the nonlinear regime

Pictorially, we see the evolution of the initial wave as it steepens and develops asymmetry in both the x and y directions. The larger velocities in the upper fluid make its momentum comparable to that of the lower fluid, despite the lower density.

Rather than roll over and break back onto the surface, as might happen in another parameter regime, here the acceleration of the liquid layer results in the development of an elongated structure. Such structures are always observed in the laboratory, at the early stages of atomization. Here we confirm their identity as the earliest strongly nonlinear structure in numerical experiments.

In actual experiments, it is at this stage that three dimensional structures typically form: ligament, or finger shaped protrusions develop from these liquid sheets, penetrating into the less dense fluid, and subsequently breaking into droplets. The breaking up of a single ligament is well described by Rayleigh's classic analysis. In these two-dimensional experiments, the sheet must break into artificial two-dimensional "drops" of infinite extent in the direction perpendicular to the page. This two-dimensional drop formation is a reduced dimension version of the usual Rayleigh mechanism, so although our experiments are artificial in their dimensionality, some validity remains because the physical breakup mechanism is the same.

REFERENCES

[1] **Lefebvre A**, *Atomization and Sprays.* Hemisphere Publ. Corp., New York, 1990
[2] **Scardovelli R & Zaleski S**, *Direct numerical simulation of free-surface and interfacial flow*, Annual Rev. of Fluid Mech. pp 567-603, 1999
[3] **Boomkamp PAM, Boersma BJ, Moesen RHM & Beijon GV**, *A Chebyshev collocation method for solving two-phase flow stability problems*, Journal of Comp. Physics 132, pp 191-200, 1997
[4] **Hooper, AP & Boyd, WGC**, *Shear-flow instability due to a wall and a viscosity difference at the interface*, JFM 179, pp.201-225, 1987
[5] **Miesen R & Boersma BJ**, *Hydrodynamic stability of a sheared liquid film*, JFM 301, pp 175-202, 1995
[6] **Hooper AP**, *The stability of two superposed viscous fluids in a channel*, Phys. Fluids A 1(7), pp1133-1142, 1989
[7] **Raynal L**, *Instabilite et entrainement a l'interface d'une couche de melange liquide-gaz*, PhD Thesis, Universite Joseph Fourier, Grenoble, 1997